International Journal of Nanomedicine

Dovepress
open access to scientific and medical research

Open Access Full Text Article

ORIGINAL RESEARCH

Effective screen for amyloid β aggregation inhibitor using amyloid β-conjugated gold nanoparticles

This article was published in the following Dove Press journal:
International Journal of Nanomedicine
14 December 2010
Number of times this article has been viewed

Sun-Ho Han[1]
Yu Jin Chang[1]
Eun Sun Jung[1]
Jong-Won Kim[2]
Duk Lyul Na[3]
Inhee Mook-Jung[1]

[1]Department of Biochemistry and Biomedical Sciences, Seoul National University, College of Medicine, Jongro-gu, Seoul, Korea; [2]Department of Laboratory Medicine and Genetics, Samsung Medical Center, Sungkyunkwan University, School of Medicine, Kangnam-Ku, Seoul, Korea; [3]Department of Neurology, Samsung Medical Center, Sungkyunkwan University, School of Medicine, Kangnam-Ku, Seoul, Korea

Abstract: The abnormal aggregation of amyloid β (Aβ) and its subsequent intra- and extracellular accumulation constitute the disease-causing cascade of Alzheimer's disease (AD). The detection of Aβ aggregates and senile plaque formation, however, is nearly impossible during early pathogenesis, and the absence of a convenient screen to validate the activity of Aβ aggregation regulators impedes the development of promising drug targets and diagnostic biomarkers for AD. Here, we conjugated amyloid β42 (Aβ42) peptide to gold nanoparticles (AuNPs) to visualize Aβ42 aggregation via Aβ42 aggregation-induced AuNP precipitation. AuNP–Aβ42 precipitate was quantified by optical density measurements of supernatants and thioflavin T binding assay. Transmission electron microscopy (TEM) analysis also showed reduced interparticle distance of AuNPs and confirmed the Aβ42 aggregation-induced AuNP precipitation. Transthyretin, a widely known Aβ aggregation inhibitor, limited AuNP–Aβ42 precipitation by preventing Aβ42 aggregation. Finally, according to TEM analysis, Aβ42-conjugated AuNPs treated with blood-driven serum revealed the differentiated aggregation patterns between normal and AD. These findings may open a scientific breakthrough in finding a possible diagnostic and prognostic tool for neurodegenerative diseases involving abnormal protein aggregation as their key pathogenesis processes.

Keywords: transthyretin, Alzheimer's disease, diagnosis, amyloid β aggregation, gold nanoparticle

Introduction

Abnormal protein aggregation is often the pivotal step in the disease-generating and propagating cascade of neurodegenerative diseases, including Alzheimer's, Parkinson's, and Huntington's diseases.[1–3] In particular, Alzheimer's disease (AD) is the most common neurodegenerative disease, and the atypical polymerization and aggregation of amyloid β (Aβ) peptide in neuronal inclusions and plaques have long been considered the hallmark of AD pathology.[3–5] The oligomeric form and senile plaques of Aβ peptide that result from aggregation are the chief causes of neuronal dysfunction, degeneration, toxicity, and, ultimately, brain malfunction, leading to malignant impairments in learning and memory in AD.[1,3,6,7]

The cleavage of amyloid precursor protein (APP) generates several Aβ species, predominantly Aβ40 and small fragments of Aβ42. Aβ42 clusters more rapidly than the former in a concentration- and temperature-dependent manner and is prone to link to intra- and extracellular deposits of Aβ aggregates, which are closely associated with the initiation of AD pathogenesis.[2,4] Specifically, recent studies have demonstrated that the oligomeric form is more closely linked to neurotoxicity and memory impairment

Correspondence: Inhee Mook-Jung
Department of Biochemistry and Biomedical Sciences, Seoul National University, College of Medicine, 28 Yungun-dong, Jongro-gu, Seoul 110-799, Korea
Tel +82 2 740 8245
Fax +82 2 3672 7352
Email inhee@snu.ac.kr

compared with the fibrillated form in senile plaques, which appears to be a secondary phenomenon following initiation.[1,3,6]

In addition to the developing amyloid hypothesis in AD, attention on Aβ aggregation inhibitors has increased in an attempt to impede aggregation. Evidence suggests that there is an endogenous inhibitor of Aβ aggregation.[8,9] Transtyretin (TTR), originally known as thyroid hormone T4 and retinol transporter, acts as an Aβ aggregation inhibitor by binding and sequestering Aβ, thereby preventing amyloidogenesis.[9,10] TTR is a homotetrameric 55-kDa protein that is produced in the liver and choroid plexus and exists in cerebrospinal fluid (CSF) and blood. Increased TTR levels in the Tg2576 mouse, an APP-overexpressing AD animal model, prevented Aβ plaque formation and neuronal loss for 12 months, despite rising Aβ levels in the brain.[10,11] Moreover, decreased TTR concentrations in CSF in human AD patients caused unbound Aβ peptide to aggregate with Aβ oligomers and plaques to form, leading to neurotoxicity and synaptic dysfunction.[12] Based on these data, TTR is a potent Aβ aggregation inhibitor and regulates AD pathogenesis.[9,12]

The combination of biomedical science and nanotechnology has launched a new era in medicine, particularly with regard to inventing and applying new treatments and diagnostic devices. Gold nanoparticles (AuNPs) have attracted much attention due to their unique properties, including amenability to particle size control, chemical composition, and surface modifications. Moreover, surface plasmon resonance (SPR) is a distinct characteristic that induces the intense red color of AuNP colloidal solutions and can be modulated based on concentration, particle size, and interparticle distance.[13,14] For 50-nm diameter AuNPs, the SPR peak develops at 520 nm, which causes the red color of this colloidal solution.[13] Further, the enormous surface area of nanoparticles enhances protein fibrillation by reducing the lag time of nucleation.[15] Much effort has been made to use AuNPs whose surfaces have been modified with nucleotides, antibodies, and drugs to sense and sequence DNA, target cancer, and mediate protein disaggregation.[14,16,17]

Here, we induced and visualized neuropathogenic Aβ42 aggregation optically by precipitating Aβ42-conjugated AuNPs. The optical density of free AuNPs (Aβ42-conjugated particles that did not precipitate) in supernatant was measured to quantify the precipitation, and thioflavin T (ThT) binding assay verified and quantified Aβ aggregation-induced AuNP precipitation. AuNP–Aβ42 precipitation occurred in a conjugated Aβ42 concentration-dependent manner and was blocked by TTR, a well known Aβ aggregation inhibitor. Moreover, this system differentiated particle distances and aggregation patterns in blood-derived samples from normal and AD patients.

Materials and methods

Preparation of AuNPs and conjugation of Aβ42 to AuNPs

Streptavidin-conjugated AuNPs (40 nm, optical density at 520 nm = 10.3, BBInternational, Cardiff, UK) were centrifuged and washed with distilled water 3 times and suspended in phosphate buffer solution (PBS) (pH = 7.2). The streptavidin–AuNP solution was combined with biotin-tagged Aβ42 (biotin–Aβ42 [H-5642.0500, Bachem, Torrance, CA, USA] dissolved in dimethyl sulfoxide [DMSO]) to a designated concentration and mixed thoroughly. The AuNP–Aβ42 solution was incubated for 48 hours at room temperature (RT) to induce aggregation.

Dot blot analysis to confirm Aβ42 conjugation to AuNP

Control (AuNPs without Aβ42) and AuNP–Aβ42 were loaded onto a nitrocellulose membrane (Protran®, Schleicher & Schuell, Keene, NH, USA) immediately after biotin–streptavidin reaction and the extensive washes with distilled water. Anti-Aβ42 (epitope: Aβ17–24 monoclonal antibody 4G8 [SIG-39220, Covance, Princeton, NJ, USA]) was used to detect Aβ42 on the surface of AuNPs, visualized using horseradish peroxidase-conjugated secondary antibody (HRP-anti-mouse IgG, Pierce, Rockford, IL, USA) in an enhanced chemiluminescence reaction (GE Healthcare, Piscataway, NJ, USA). Images were taken on Las-3000 (Fuji Film, Tokyo, Japan).

Optical density measurements and ThT binding assay

The optical density of the supernatant was measured at 520 nm on a spectrophotometer (ND-1000, NanoDrop, Wilmington, DE, USA). For the ThT binding assay, 20 μL of sample was mixed with 150 μL of 5 μmol/L Thioflavin T solution in 50 mmol/L glycine buffer, and the fluorescence was measured within 15 minutes (Infinite M200, TECAN, Switzerland, excitation 437, emission 485 nm).

Blood-derived serum preparation

Blood (3 mL) from normal and AD patients was provided by Samsung Medical Center with approval from the local ethical review board; informed consent was obtained from all subjects. Vaccutainers (Vacuette [#450076, Greimer Bio-One, Monroe, NC, USA]) and SST tubes (SSTTMII

Advance [#368972, Becton, Dickinson and Company, Franklin, NJ, USA]) were used to collect blood. Inside the SST tube, serum was separated by serum separation gel, and the upper serum layer was drawn and stored at −80°C.

Preparation and quantification of human serum TTR level

TTR was purchased from Sigma-Aldrich (St Louis, MO, USA), suspended and diluted in PBS (pH = 7.2), and incubated with AuNP–Aβ42 solution for 48 hours at RT. Human TTR levels in serum were measured using a human prealbumin detection enzyme-linked-immunosorbent serologic assay (ELISA) kit (Standard Diagnostic, Inc., Kyunggi-do, Korea) according to the manufacturer's guidelines. In brief, human sera were diluted with sample diluents 1:4000 (working on ice), loaded onto plates coated with human TTR-specific antibody (DAKO, Glostrup, Denmark) and incubated for 30 minutes at 37°C. They were then washed five times and incubated with HRP-conjugated human TTR-specific antibody (Standard Diagnostic, Inc., Kyunggi-do, Korea) for 30 minutes at 37°C. After being washed a further five times, stabilized TMB (3,3′,5,5′-tetramethylbenzidine) solution was added for 10 minutes at RT, and then stop solution was added. Absorbance at 450 nm was read using a plate reader (POWER-XS, BIO-TEK, Vinooski, VT, USA).

TEM analysis

AuNP–Aβ42 was prepared as described above; 1 drop (10 μL) of solution was mounted on a carbon-coated grid (200 mesh, Electron Microscopy Science, PA, USA). Two hours after filtering and drying at RT, TEM images were taken and analyzed on a JEM-1400 (Jeol, Tokyo, Japan).

Statistical analysis

All data were expressed as mean ± SEM (standard error of the mean) or fold-change of the mean compared with control. Student *t*-test was used for two-group comparisons, and analysis of variance, followed by Tukey-Kramer multiple comparison test, was used to compare three or more groups. Significance was designated as P-value < 0.05.

Results

Conjugation of Aβ peptide to AuNP and visualization of Aβ aggregation-induced AuNP precipitation

In this initial step, we hypothesized that it would be possible to visualize protein aggregation if we conjugated Aβ peptides to the surface of nanoparticles that had distinct colors or characteristics (Figure 1). AuNPs in a colloidal solution have a unique red color due to SPR; the color is altered by changes in particle size, distance, and concentration.[18] Aβ42 peptide was conjugated to AuNP (40 nm) by streptavidin–biotin reaction and then incubated for 48 hours at RT for inducing Aβ42 aggregation. The AuNP control was added to an equal amount of DMSO vehicle. Aβ42 conjugation to the AuNP was confirmed by dot blot analysis (Figure 2A). The AuNP control (without Aβ42 conjugation) failed to generate a signal, whereas AuNP–Aβ42 elicited a robust positive signal from anti-Aβ42.

Incubation at RT for 48 hours induced a visible purple precipitate and a clear supernatant in the AuNP–Aβ42 solution but not for unconjugated AuNP (Figure 2B). AuNPs had a distinct red color in colloidal solution, and AuNP–Aβ42 precipitation was observed, as was a clearer supernatant than the AuNP control, due to the decreased concentration of free AuNPs. Changes in interparticle distance in AuNPs in the precipitate caused the color to change from red to purple and induced a thin, tightly packed layer of precipitate on the bottom of the tube.

The optical density of the supernatant at 520 nm (the property of AuNP that confers their red color) was measured and compared as a quantitative indicator of the amount of AuNP–Aβ42 precipitation. The supernatant of the AuNP–Aβ42 solution had a lower optical density than the unconjugated AuNP control ($P < 0.0001$) (Figure 2C), due to the AuNP–Aβ42 precipitate. By ThT binding assay, β-sheet-enriched Aβ42 aggregates were detected in the AuNP–Aβ42 precipitate, demonstrating that precipitation resulted from Aβ42 aggregation ($P < 0.005$) (Figure 2D); the ThT binding assay is routinely and frequently used to measure and quantify Aβ42 aggregation.[19] AuNP–Aβ42 precipitation caused a 238% increase in ThT values compared with the AuNP control. A time-dependent increase of aggregation and precipitation of AuNP–Aβ42 was investigated, and 48-hour incubation was the time point at which to maximize the reaction (Supplementary Figure 1).

Aβ42 concentration-dependent increase in AuNP–Aβ42 precipitation

We determined whether the amount of AuNP–Aβ42 precipitation was proportional to the concentration of Aβ42 that was conjugated to AuNPs. Biotin–Aβ42, at concentrations ranging from 0 to 300 μmol/L, was conjugated to AuNPs and incubated for 48 hours to induce precipitation. Based on the optical density and ThT binding assay results, AuNP–Aβ42 precipitation and Aβ42

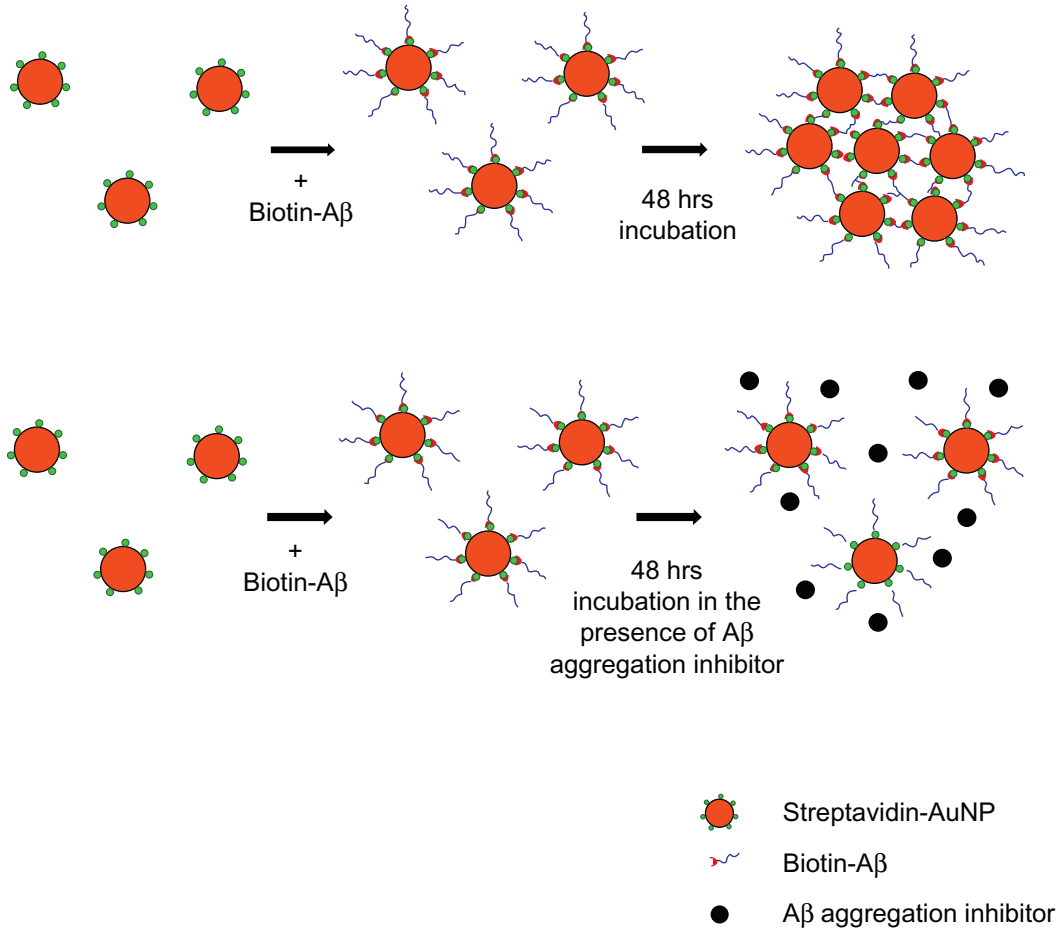

Figure 1 Schematic of sequence of Aβ42 conjugation to AuNP surface via biotin–streptavidin interaction and formation of AuNP–Aβ42 precipitate by Aβ42 aggregation.
Abbreviations: Aβ, amyloid β; Aβ42, amyloid β42; AuNP, gold nanoparticle.

aggregation increased in an Aβ42 concentration-dependent manner (Figure 3). AuNP–Aβ42 precipitation was visible between 10 and 50 μmol/L Aβ42, consistent with the results of the optical density and ThT binding assays, which demonstrated lower optical density and increased ThT binding, respectively, at 50 μmol/L.

Thus, the simultaneous changes in visual precipitation, optical density, and ThT binding at 50 μmol/L Aβ42 suggest that AuNP–Aβ42 precipitation is caused by Aβ42 aggregation. Above 50 μmol/L, the optical density pattern reversed, despite the increase in ThT binding (100, 300 μmol/L). We speculated that residual-free biotin–Aβ42 in the solution incorporated into AuNP–Aβ42 precipitates during aggregation and expanded the interparticle distance, exceeding that in AuNP–Aβ42 that did not contain extra biotin–Aβ42 (50 μmol/L) but remaining shorter than in the AuNP control. The appearance of AuNP–Aβ42 precipitates in 300 μmol/L biotin–Aβ42 in Figure 3A supports this model, because its aggregation pattern differed compared with 50 μmol/L, developing a dark purple, cloudy, and floating precipitate rather than a tight, thin layer. We believe that these floating AuNP–Aβ42 aggregate particles influenced the optical density measurements and increased the optical density; thus, the optimal biotin–Aβ42 concentration for AuNP conjugation was 10–50 μmol/L, and we used this range for the remaining experiments, unless noted otherwise.

Inhibition of AuNP–Aβ42 precipitation by cotreatment with the Aβ aggregation inhibitor TTR

Because Aβ42 aggregation led to AuNP–Aβ42 precipitation, we examined whether we could use this system to evaluate the activity of an Aβ42 aggregation inhibitor. Aβ42 aggregation inhibitors prevent and alleviate Aβ42 aggregation, regulating AD pathogenesis.[8,12] Based on increased Aβ deposits due to TTR mutation or deficiency, TTR is considered an Aβ aggregation inhibitor and governs AD pathogenesis.[11,20] We incubated AuNP–Aβ42 with or without TTR (3 μmol/L, Sigma) for 48 hours and observed that TTR inhibited AuNP–Aβ42 aggregation, eliciting no visible precipitation and generating

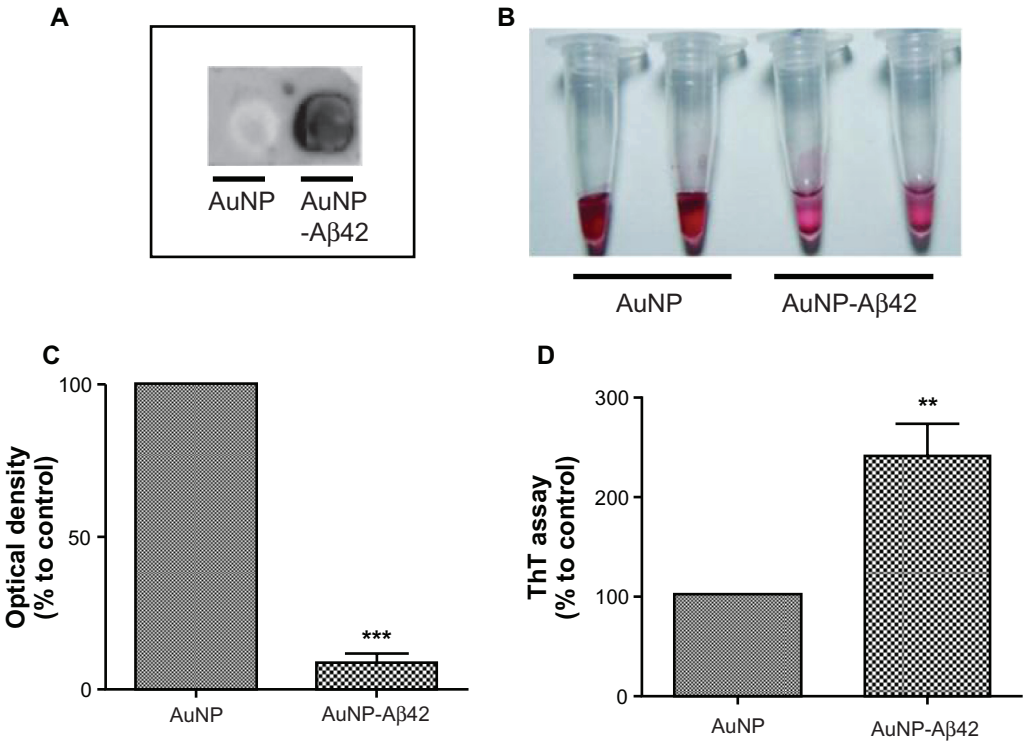

Figure 2 Confirmation of Aβ42 conjugation to AuNP and induction of AuNP–Aβ42 precipitates by Aβ42 aggregation. **A**) Verification of biotin–Aβ42 conjugation to streptavidin-AuNP by dot blot analysis. **B**) After 48 hours incubation, visible AuNP–Aβ42 precipitates formed in the bottom of the tubes and the supernatant became clear; no precipitate was observed in the AuNP control. **C**) Optical density of supernatant as a quantitative indicator of AuNP–Aβ42 precipitation (Paired *t*-test, $^{***}P < 0.0001$). **D**) ThT binding assay to measure and quantify Aβ42 aggregation, reflected by significantly increased ThT binding in AuNP–Aβ42 ($^{**}P < 0.005$).
Abbreviations: Aβ42, amyloid β42; AuNP, gold nanoparticle; ThT, thioflavin T.

a completely different color in the supernatant compared with AuNP–Aβ42 (Figure 4A). TTR rescued the decrease in optical density and increase in ThT binding in AuNP–Aβ42 by inhibiting Aβ42 aggregation (Figure 4B and 4C).

By TEM, the particle arrangement of AuNP–Aβ42 precipitate was identified, as was its change on TTR inhibition of Aβ aggregation. The AuNP–Aβ42 preparation was the same as in the previous experiment. The same concentrations and volumes of AuNP, free Aβ42 (50 μmol/L, Aβ42 without biotin, American Peptide, Sunnyvale, CA), TTR (3 μmol/L, Sigma) were used for each set. Unconjugated AuNP did not cluster and dispersed homogeneously, whereas AuNP–Aβ42 assembled and clustered, distributing itself heterogeneously (Figure 5A). Particle distances fell significantly in AuNP–Aβ42 aggregates, compared with AuNP without Aβ42 conjugation ($P < 0.001$) (Figure 5A and 5B). Small gaps between particles in AuNP–Aβ42 were possible spaces for conjugated Aβ42 to aggregate. Incubation of AuNP–Aβ42 with additional free Aβ42 led to the same pattern of precipitation as with 300 μmol/L biotin–Aβ42 in Figure 3, which formed floating dark purple granules (Supplementary Figure 2). The distances between particles were greater than in AuNP–Aβ42 aggregates but shorter than the AuNP control, and the background appeared dark and irregular, possibly reflecting the aggregation of free Aβ42. Incubation of AuNP–Aβ42 with TTR for 48 hours did not cause precipitation or clustering of AuNP–Aβ42, and the particles were distributed evenly, as in the control, due to the inhibition of aggregation by TTR (Figure 5A and 5B, Supplementary Figure 2). There was no difference from the AuNP control and a significant increase compared with AuNP–Aβ42 ($P < 0.001$) with regard to particle distance, and background staining did not develop. TTR had no direct effect on AuNPs when they were added with TTR (Supplementary Figure 2). These results suggest that this AuNP–Aβ42 system is a potential method for screening candidates of Aβ42 aggregation inhibitors. Visualizing AuNP–Aβ42 precipitation would be a tremendous advantage in validating inhibitor activities and specificities.

Differential aggregation patterns of AuNP–Aβ42 in sera from normal and AD patients

We hypothesized that this system could be used for blood-derived samples to differentiate AD patients from normal individuals by monitoring AuNP–Aβ42 aggregation. Serum (1/20 dilution) from four AD patients and four normal controls

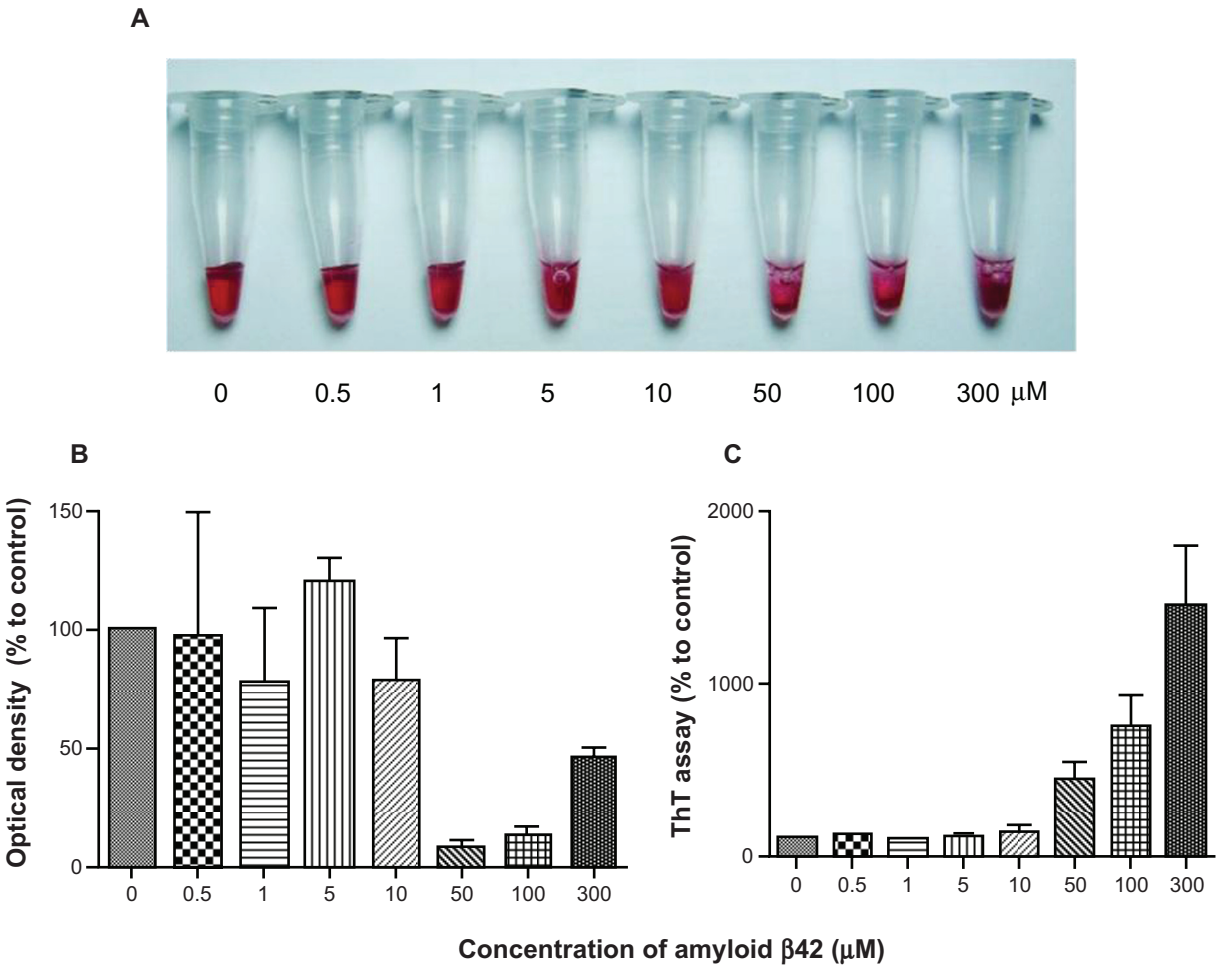

Figure 3 AuNP–Aβ42 precipitates in an Aβ42 concentration-dependent manner. Various concentrations of biotin–Aβ42 (0, 0.5, 1, 5, 10, 50, 100, and 300 μmol/L) were added to streptavidin-AuNP to determine the optimal concentration of Aβ42 conjugation. Visible precipitates developed at 50 μmol/L biotin–Aβ42 **A**), accompanied by a decrease in optical density **B**), and increase in ThT binding **C**), indicating that 10–50 μmol/L is the optimal concentration of Aβ42 to saturate AuNP surfaces and induce AuNP–Aβ42 aggregation. Above 50 μmol/L, free Aβ42 reverses the optical density despite the increased ThT value.
Abbreviations: Aβ42, amyloid β42; AuNP, gold nanoparticle; ThT, thioflavin T.

was tested. The average ages of control and AD subjects were 71 ± 2.00 and 80 ± 3.65 years, respectively. Serum TTR levels were also quantified and compared, showing 1227.25 ± 18.30 in the control and 408.25 ± 75.33 in the AD group, respectively. Although it was hard to tell the clear differences in AuNP–Aβ42 precipitation patterns (Supplementary Figure 3), TEM images showed increased AuNP–Aβ42 aggregation in AD serum and relatively even distribution of particles in the normal controls (Figure 6A and 6B). The background developed irregular patterns of protein aggregation in both normal and AD patients. In normal serum, AuNP–Aβ42 spread evenly, yet AuNP–Aβ42 in AD serum clustered near or above the protein aggregate, reflected by the dark background staining. Moreover, Figure 6B shows differential patterns of AuNP–Aβ42 aggregation between normal and AD individuals, revealing that the interparticle distance was significantly shortened in AD compared with normal samples. In AD samples, particles clustered near the protein aggregation of dark-stained background, whereas homogeneous dispersion was shown in normal subjects.

Discussion

We have demonstrated that the combination of two distinct properties – the color of visible precipitates of AuNPs and the aggregation-prone nature of Aβ – makes the visualization of Aβ aggregation possible. The strong conjugation of Aβ42 to AuNP by biotin–streptavidin interaction, followed by a 48-hour incubation in PBS (pH = 7.2), induced aggregation, which was detected easily as dark purple precipitation.

Kogan et al reported that 10 nm β sheet breaker (PEP)-conjugated AuNP recognized and bound the hydrophobic pocket of Aβ42 and formed small black precipitates after 168 hours at 37°C.[17] Their purpose in inducing hydrophobic aggregation between AuNP–PEP and Aβ was to use AuNPs

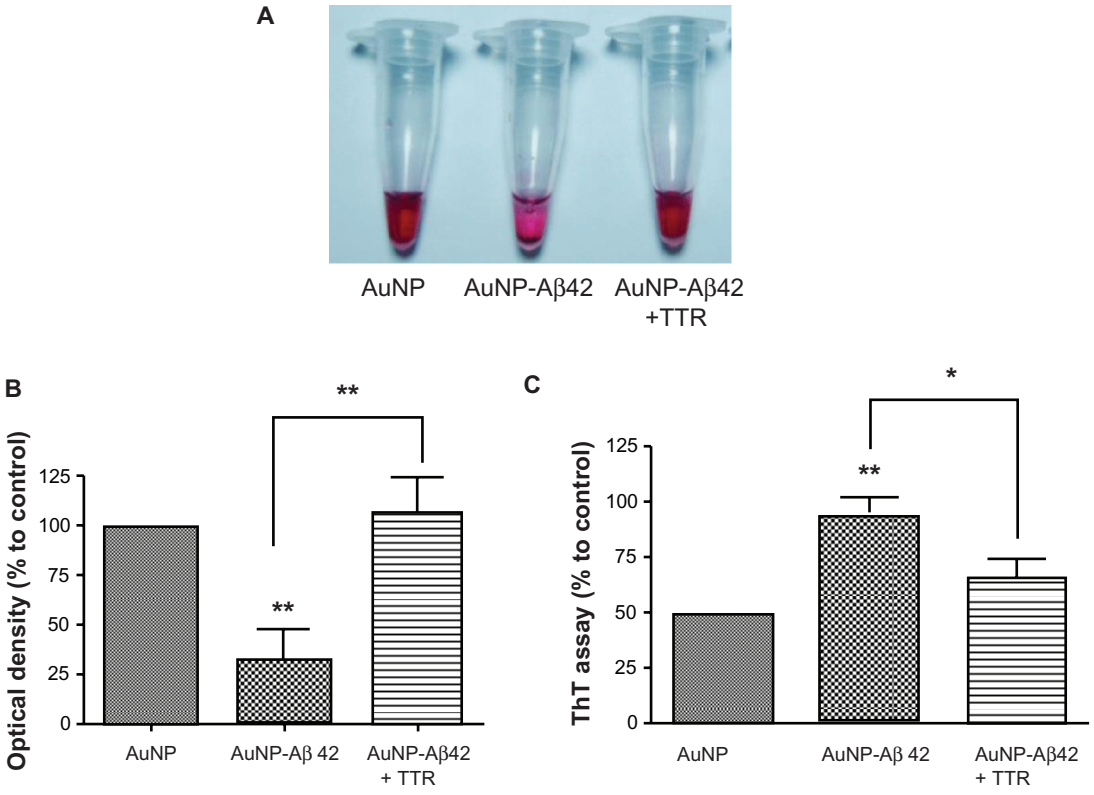

Figure 4 Activity validation of an Aβ aggregation inhibitor TTR, using AuNP–Aβ42 precipitates. In inducing AuNP–Aβ42 aggregation, its coincubation with TTR prevented the formation of visible AuNP–Aβ42 precipitates and maintained the red color of the colloidal solution, as in the AuNP control **A**). TTR reversed the significant decrease in optical density **B**), and increase in ThT value **C**) of AuNP–Aβ42, resulting from the inhibition of both Aβ aggregation and AuNP–Aβ42 and one-way ANOVA (*$P < 0.05$, **$P < 0.01$).
Abbreviations: Aβ, amyloid β; Aβ42, amyloid β42; AuNP, gold nanoparticle; ThT, thioflavin T; TTR, transtyretin.

to mediate the delivery of irradiation to Aβ aggregates, demonstrating the dissolution of Aβ precipitate and the reappearance of the red AuNP solution by irradiation. However, the precipitate was rarely visible, and 168 hours is a long period to wait to induce protein aggregation.

Thus, we conjugated full-length Aβ42 directly to AuNP through strong interactions of biotin–streptavidin. This specific conjugation fastened aggregation and precipitation only after 48 hours at RT, allowing us to quantify and compare AuNP–Aβ42 precipitates. Protein aggregation and fibril formation have nucleation-dependent kinetics; thus, Aβ42 nucleation appears to be the rate-limiting step of aggregation and fibrillation. Nanoparticles may initiate protein nucleation and reduce nucleation lag time.[15]

Our results in Figure 2 show that the attachment of Aβ42 to nanoparticles induced aggregation in a relatively short time (48 hours), compared with 168 hours in Kogan et al's experiments. Also, it is noted that the appearance of AuNP–Aβ42 precipitates induced by full-length Aβ42 aggregation in our study differed from the hydrophobic incorporation of small-fragment Aβ42 to full-length Aβ42. Factors such as size of nanoparticle, types, and length of Aβ and conjugation method might affect the appearance of this precipitate.

This visible AuNP–Aβ42 precipitate system is useful in screening and validating possible drug targets and diagnostic approaches. TTR, a well known Aβ42 aggregation inhibitor, had no direct influence on AuNP itself (Supplementary Figure 2), but it blocked AuNP–Aβ42 precipitation by inhibiting Aβ42 aggregation (Figure 4). The possible explanation for this phenomenon is that TTR binds to Aβ42 and blocks the initial nucleation of Aβ42 aggregation, which prohibits further processing. We incubated AuNP–Aβ42 and TTR for up to 168 hours and did not observe any difference.

The TEM analysis in Figure 5 details the structure and interparticle distances of AuNP–Aβ42 precipitates and TTR activity. AuNP–Aβ42+TTR affected a particle distance and distribution that were similar to those in AuNP control, but AuNP–Aβ42 alone clustered in an irregular pattern. As discussed, AuNP–Aβ42+free Aβ42 clustered and precipitated in a pattern that differed from AuNP–Aβ42. Additional free Aβ42 lengthened the particle distance compared with AuNP–Aβ42 aggregates but remained shorter than the AuNP control. Also, the addition of free Aβ42 to AuNP–Aβ42

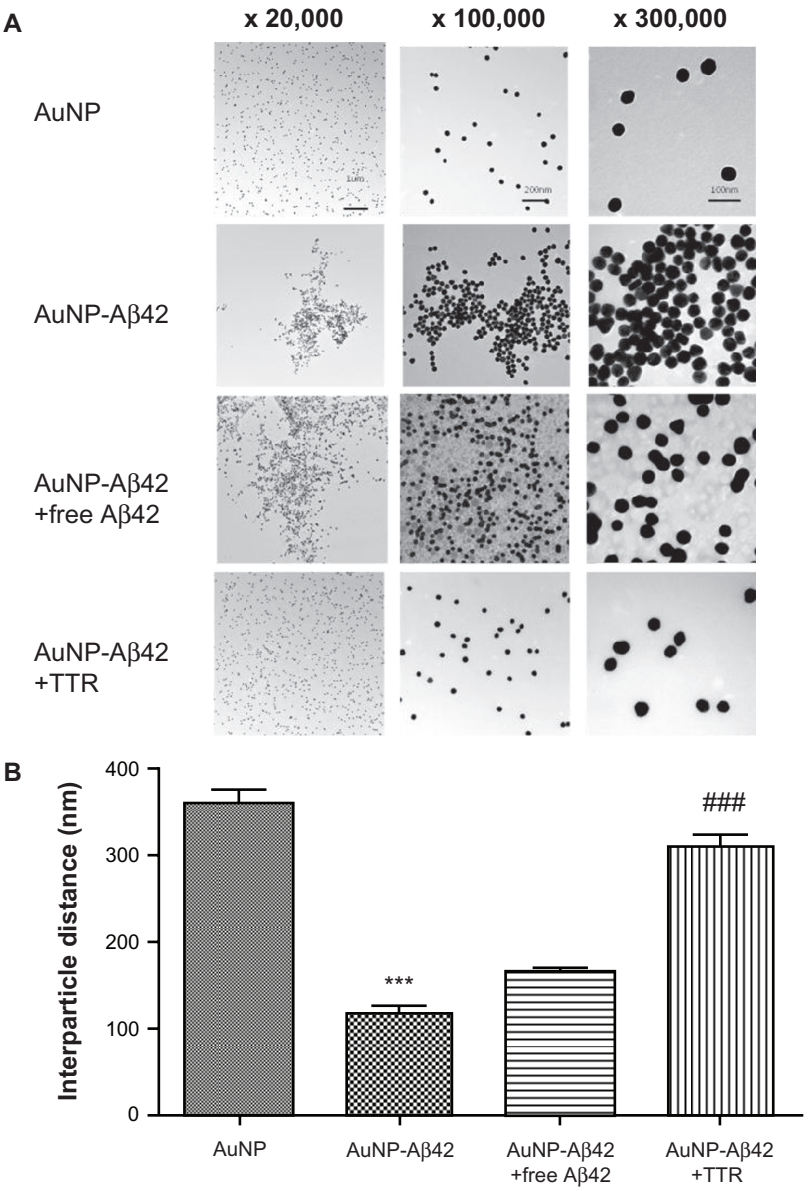

Figure 5 TEM analysis of AuNP–Aβ42 precipitates. **A**) AuNP–Aβ42 formed clusters with short interparticle distances, and AuNP underwent an even distribution of particles. The addition of free Aβ42 resulted in a similar pattern of aggregation as AuNP–Aβ42 but a greater interparticle distance and dark background staining. TTR blocked the formation of AuNP–Aβ42 aggregates and maintained the homogeneous dispersion of particles as evenly as the AuNP control. **B**) Interparticle distances were measured and compared (***$P < 0.001$ compared with AuNP, ###$P < 0.001$ compared with AuNP–Aβ42).
Abbreviations: Aβ42, amyloid β42; AuNP, gold nanoparticle; TEM, transmission electron microscopy; TTR, transtyretin.

(AuNP–Aβ42+free Aβ42) induced a dark background of protein that did not appear in AuNP–Aβ42 (Figure 5A). This result might have been caused by the intervention of free Aβ42 into AuNP–Aβ42 aggregates during precipitation, and the irregular background staining reflects Aβ42 aggregation between AuNP–Aβ42 and free Aβ42. Also, based on this result, we are reassured that AuNP–Aβ42 precipitate is caused by aggregation of "unfree" biotin–Aβ42 but conjugated Aβ42 to AuNP. We might be able to use these distinct characteristics of AuNP–Aβ42 precipitates in the presence of free Aβ42 to detect and quantify free Aβ42 by adjusting the proportion of conjugated and free Aβ42 in future studies. At certain concentration ratios – possibly a lower biotin–Aβ42 concentration than what is used to saturate AuNP surfaces (50 μmol/L) – free Aβ42 might lead to aggregation and precipitation that are proportional to the free Aβ42 concentration.

Levels of protein aggregates, appearing as background staining by TEM, peaked in blood-derived serum samples (Figure 6). High concentrations of diverse proteins in serum and the nonspecific intercalation of AuNP–Aβ42 into serum protein aggregates meant that it was not possible to see a clear difference in AuNP–Aβ42 precipitates between normal

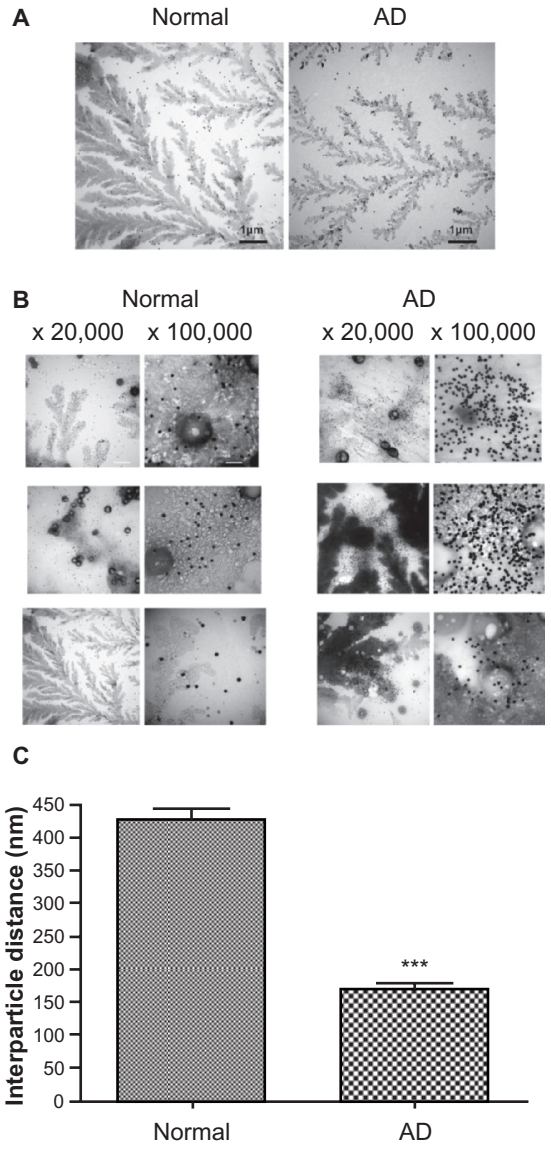

Figure 6 TEM analysis of AuNP–Aβ42 incubated with blood-derived serum from normal and AD patients. Sera from normal individuals (n = 4) and AD patients (n = 4) were incubated with AuNP–Aβ42 during aggregation. AuNP–Aβ42 in AD patient serum showed aggregation and significantly shorter interparticle distances (**A** right, **B** right, and **C**) (***$P < 0.001$), whereas AuNP–Aβ42 in normal serum dispersed evenly and represent regular distances (**A** left, **B** left, and **C**). Sera from both normal and AD patients developed irregular and dark backgrounds of protein aggregation (white scale bar in × 20,000 image: 200 μm, in × 100,000 image: 200 nm).
Abbreviations: AD, Alzheimer's disease; Aβ42, amyloid β42; AuNP, gold nanoparticle; TEM, transmission electron microscopy.

and AD-derived sera, yet TEM analysis clearly showed differential patterns of particle distance and aggregation. Compared with normal samples, AD serum that was incubated with AuNP–Aβ42 developed AuNP–Aβ42 clusters with significantly short particle distances; most aggregates were concentrated in the dark protein aggregation background stain. This result might be explained by several mechanisms. First, the concentration of Aβ42 aggregation inhibitor might be lower in AD blood compared with normal subjects. As shown in Figure 4, TTR is a known active Aβ42 aggregation inhibitor that exists in low concentrations in CSF of AD patients.[12] We confirmed the concentration of TTR in blood-derived serum, quantified by ELISA, and demonstrated significantly lower concentrations in AD subjects compared with the normal group. Besides TTR, the possibility of the existence of AD-related changes of other Aβ binding proteins could not be excluded. The potential role of metal ions has been reported in Aβ aggregation and AD pathogenesis. Metal ions, such as copper and zinc, bind to Aβ42, and their concentrations are susceptible to change during AD pathogenesis.[21] Metal ions, especially copper and zinc, bind and induce Aβ42 aggregation, and their concentration in blood might change during the pathogenic process and influence Aβ42 aggregation.[22,23] Other factors that might govern Aβ42 aggregation should be considered, including biological lipids, which have been reported to generate toxic Aβ42 protofibrils.[24]

Conclusion

We visualized Aβ42 aggregation through the conjugation of Aβ42 to AuNPs. AuNP–Aβ42 precipitate was quantified by optical density measurements of AuNP supernatant and ThT binding assay. With this method, an Aβ42 aggregation inhibitor screen was performed and successfully validated the effect of TTR against AuNP–Aβ42 aggregation. Our TEM analysis supported these results and further differentiated between aggregation patterns of AuNP–Aβ42 in AD blood and normal controls. These findings establish a valuable screening system for Aβ aggregation regulators and potentiate the development of diagnostic and prognostic tools for neurodegenerative diseases in which abnormal protein aggregation is the critical step in their pathogenesis.

Acknowledgment

This project was funded by grants from the 21C Frontier Functional Proteomics Project (FPR08K1301-02210), NRF 2009-0081673, WCU-Neurocytomics, Basic Research Program (2008-05943) of NRF, and the KNIH R&D program project (2009-0443) for IMJ.

Disclosure

The authors report no conflicts of interest in this work.

References

1. Lesne S, Koh MT, Kotilinek L, et al. A specific amyloid-beta protein assembly in the brain impairs memory. *Nature*. 2006;440:352–357.
2. Mucke L. Neuroscience: Alzheimer's disease. *Nature*. 2009;461:895–897.
3. Taylor JP, Hardy J, Fischbeck KH. Toxic proteins in neurodegenerative disease. *Science*. 2002;296:1991–1995.

4. Hardy J, Selkoe DJ. The amyloid hypothesis of Alzheimer's disease: progress and problems on the road to therapeutics. *Science*. 2002;297: 353–356.
5. Holtzman DM. Alzheimer's disease: moving towards a vaccine. *Nature*. 2008;454:418–420.
6. Walsh DM, Klyubin I, Fadeeva JV, et al. Naturally secreted oligomers of amyloid beta protein potently inhibit hippocampal long-term potentiation in vivo. *Nature*. 2002;416:535–539.
7. Meyer-Luehmann M, Spires-Jones TL, Prada C, et al. Rapid appearance and local toxicity of amyloid-beta plaques in a mouse model of Alzheimer's disease. *Nature*. 2008;451:720–724.
8. Bohrmann B, Tjernberg L, Kuner P, et al. Endogenous proteins controlling amyloid beta-peptide polymerization. Possible implications for beta-amyloid formation in the central nervous system and in peripheral tissues. *J Biol Chem*. 1999;274:15990–15995.
9. Costa R, Ferreira-da-Silva F, Saraiva MJ, Cardoso I. Transthyretin protects against A-beta peptide toxicity by proteolytic cleavage of the peptide: a mechanism sensitive to the Kunitz protease inhibitor. *PLoS One*. 2008;3:e2899.
10. Schwarzman AL, Gregori L, Vitek MP, et al. Transthyretin sequesters amyloid beta protein and prevents amyloid formation. *Proc Natl Acad Sci U S A*. 1994;91:8368–8372.
11. Stein TD, Johnson JA. Lack of neurodegeneration in transgenic mice overexpressing mutant amyloid precursor protein is associated with increased levels of transthyretin and the activation of cell survival pathways. *J Neurosci*. 2002;22:7380–7388.
12. Hansson SF, Andreasson U, Wall M, et al. Reduced levels of amyloid-beta-binding proteins in cerebrospinal fluid from Alzheimer's disease patients. *J Alzheimers Dis*. 2009;16:389–397.
13. Hu M, Chen J, Li ZY, et al. Gold nanostructures: engineering their plasmonic properties for biomedical applications. *Chem Soc Rev*. 2006; 35:1084–1094.
14. Mirkin CA, Letsinger RL, Mucic RC, Storhoff JJ. A DNA-based method for rationally assembling nanoparticles into macroscopic materials. *Nature*. 1996;382:607–609.
15. Linse S, Cabaleiro-Lago C, Xue WF, et al. Nucleation of protein fibrillation by nanoparticles. *Proc Natl Acad Sci U S A*. 2007;104: 8691–8696.
16. Eghtedari M, Liopo AV, Copland JA, Oraevsky AA, Motamedi M. Engineering of hetero-functional gold nanorods for the in vivo molecular targeting of breast cancer cells. *Nano Lett*. 2009;9: 287–291.
17. Kogan MJ, Bastus NG, Amigo R, et al. Nanoparticle-mediated local and remote manipulation of protein aggregation. *Nano Lett*. 2006;6: 110–115.
18. Boisselier E, Astruc D. Gold nanoparticles in nanomedicine: preparations, imaging, diagnostics, therapies and toxicity. *Chem Soc Rev*. 2009; 38:1759–1782.
19. Groenning M, Olsen L, van de Weert M, Flink JM, Frokjaer S, Jorgensen FS. Study on the binding of Thioflavin T to beta-sheet-rich and non-beta-sheet cavities. *J Struct Biol*. 2007;158: 358–369.
20. Sousa MM, Cardoso I, Fernandes R, Guimaraes A, Saraiva MJ. Deposition of transthyretin in early stages of familial amyloidotic polyneuropathy: evidence for toxicity of nonfibrillar aggregates. *Am J Pathol*. 2001;159:1993–2000.
21. Lovell MA, Robertson JD, Teesdale WJ, Campbell JL, Markesbery WR. Copper, iron and zinc in Alzheimer's disease senile plaques. *J Neurol Sci*. 1998;158:47–52.
22. Curtain CC, Ali F, Volitakis I, et al. Alzheimer's disease amyloid-beta binds copper and zinc to generate an allosterically ordered membrane-penetrating structure containing superoxide dismutase-like subunits. *J Biol Chem*. 2001;276:20466–20473.
23. Atwood CS, Moir RD, Huang X, et al. Dramatic aggregation of Alzheimer abeta by Cu(II) is induced by conditions representing physiological acidosis. *J Biol Chem*. 1998;273:12817–12826.
24. Martins IC, Kuperstein I, Wilkinson H, et al. Lipids revert inert Abeta amyloid fibrils to neurotoxic protofibrils that affect learning in mice. *EMBO J*. 2008;27:224–233.

Supplementary figures

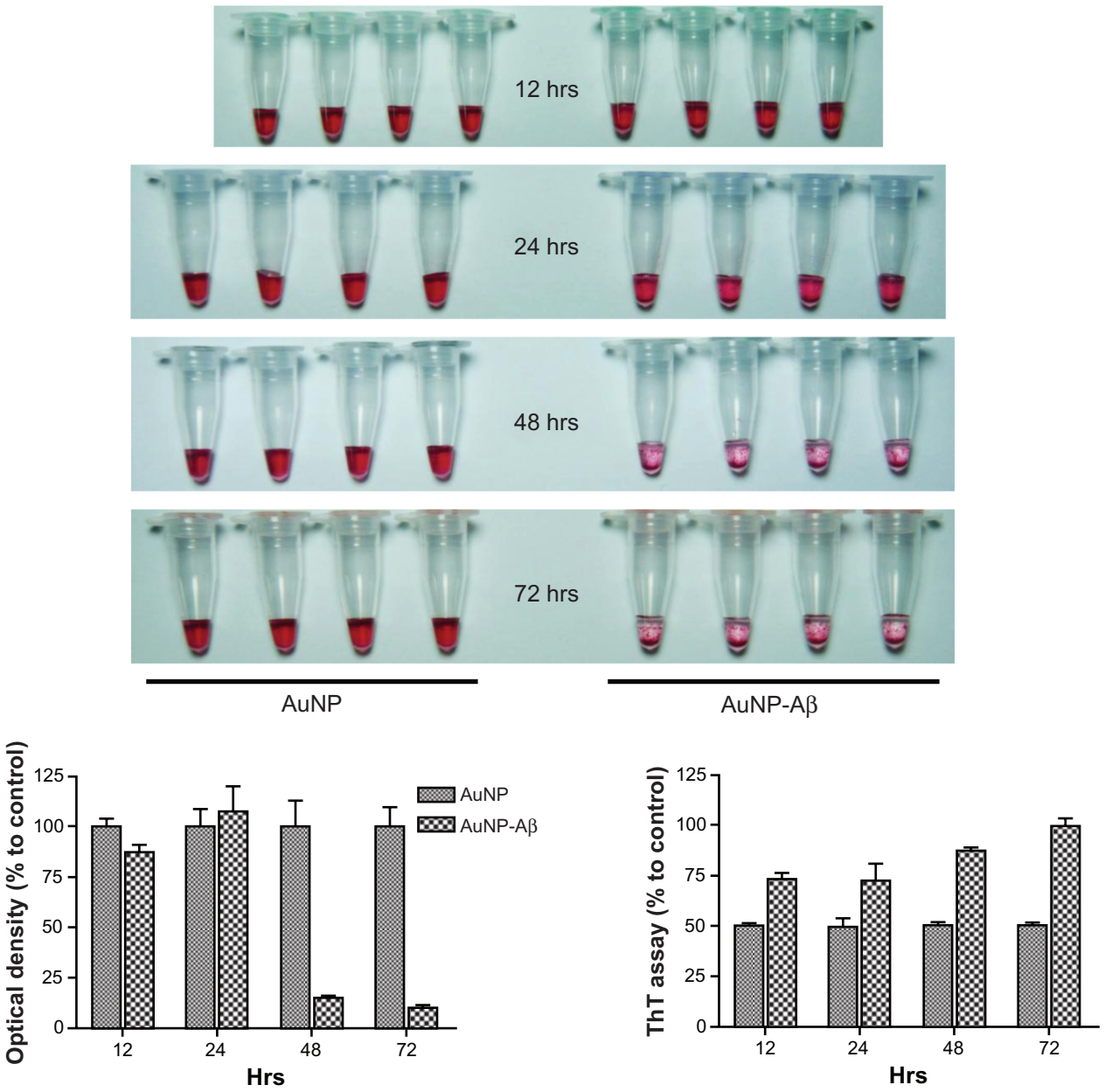

Figure S1 Time-dependent aggregation and precipitation pattern of AuNP–Aβ42.
Abbreviations: Aβ, amyloid β; Aβ42, amyloid β42; AuNP, gold nanoparticle; ThT, thioflavin T.

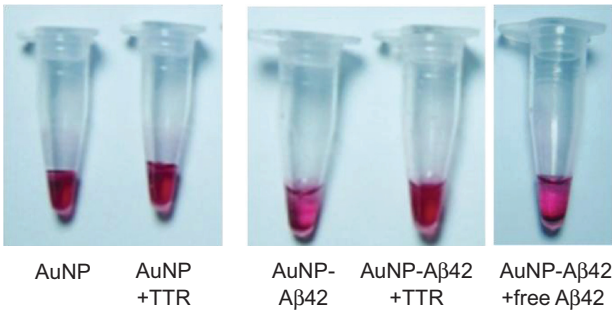

Figure S2 Precipitation pattern of AuNP–Aβ42 with or without TTR or free Aβ42. Images were taken before the TEM analysis in Figure 5.
Abbreviations: Aβ42, amyloid β42; AuNP, gold nanoparticle; TEM, transmission electron microscopy; TTR, transtyretin.

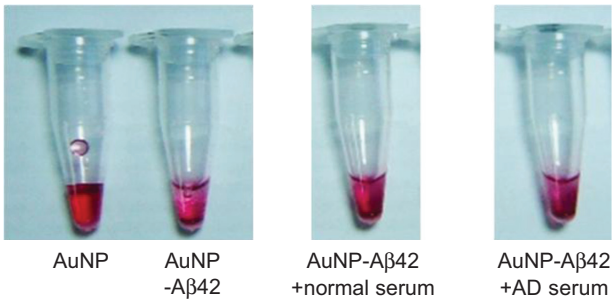

Figure S3 Precipitation pattern of AuNP–Aβ42 incubated with sera from normal and AD patients. Images were taken before TEM analysis in Figure 6.
Abbreviations: AD, Alzheimer's disease; Aβ42, amyloid β42; AuNP, gold nanoparticle; TEM, transmission electron microscopy.